

Document downloaded from the institutional repository of the University of Alcalá: <https://ebuah.uah.es/dspace/>

This is a postprint version of the following published document:

García-Castro, M. et al., 2019. The Puzzling Monopentamethylcyclopentadienyltitanium(III) Dichloride Reagent: Structure and Properties. *Inorganic chemistry*, 58(8), pp.5314–5324.

Available at <https://doi.org/10.1021/acs.inorgchem.9b00437>

© 2019 American Chemical Society.

(Article begins on next page)



This work is licensed under a
Creative Commons Attribution-NonCommercial-NoDerivatives
4.0 International License.

The Puzzling Monopentamethylcyclopentadienyltitanium(III) Dichloride Reagent: Structure and Properties

María García-Castro,[†] Cristina García-Iriepa,^{‡,⊥} Estefanía del Horno,[†] Avelino Martín,^{†,||}
Miguel Mena,^{†,||} Adrián Pérez-Redondo,^{†,||} Manuel Temprado,^{*,‡,||} and Carlos Yélamos^{*,†,||}

[†] Departamento de Química Orgánica y Química Inorgánica, Universidad de Alcalá. 28805
Alcalá de Henares-Madrid (Spain). E-mail: carlos.yelamos@uah.es

[‡] Departamento de Química Analítica, Química Física e Ingeniería Química, Universidad
de Alcalá. 28805 Alcalá de Henares-Madrid (Spain). E-mail: manuel.temprado@uah.es

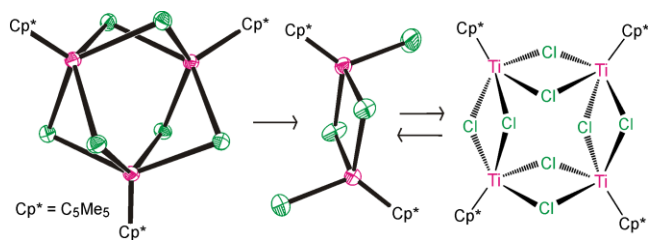
[⊥] Departamento de Química, Universidad de La Rioja, Centro de Investigación en Síntesis
Química (CISQ), 26006 Logroño (Spain)

^{||} Instituto de Investigación Química “Andrés M. del Río” (IQAR), Universidad de Alcalá.
28805 Alcalá de Henares-Madrid (Spain).

Dedicated to the memory of Prof. Dr. Pascual Royo, who passed away in July 2018

Synopsis:

Dimeric [$\{\text{Ti}(\eta^5\text{-C}_5\text{Me}_5)\text{Cl}(\mu\text{-Cl})\}_2$] and trimeric [$\{\text{Ti}(\eta^5\text{-C}_5\text{Me}_5)(\mu\text{-Cl})_2\}_3$] aggregates have been structurally characterized. CASPT2//CASSCF and BS DFT calculations support the singlet character of the dimer and a relatively large singlet-triplet energy gap. However, in hydrocarbon solutions, the dimer could establish an equilibrium with a paramagnetic tetramer [$\{\text{Ti}(\eta^5\text{-C}_5\text{Me}_5)(\mu\text{-Cl})_2\}_4$] according to NMR and computational studies.



Abstract:

Following the track of the useful titanocene $[\text{Ti}(\eta^5\text{-C}_5\text{H}_5)_2\text{Cl}]$ reagent in organic synthesis, the related half-sandwich titanium(III) derivatives $[\text{Ti}(\eta^5\text{-C}_5\text{R}_5)\text{Cl}_2]$ are receiving increasing attention in radical chemistry of many catalyzed transformations. However, the structure of the active titanium(III) species remains unknown in the literature. Herein, we describe the synthesis, crystal structure, and electronic structure of titanium(III) aggregates of composition $[\{\text{Ti}(\eta^5\text{-C}_5\text{Me}_5)\text{Cl}_2\}_n]$. The thermolysis of $[\text{Ti}(\eta^5\text{-C}_5\text{Me}_5)\text{Cl}_2\text{Me}]$ (**1**) in benzene or hexane at 180 °C results in the clean formation of $[\{\text{Ti}(\eta^5\text{-C}_5\text{Me}_5)\text{Cl}(\mu\text{-Cl})_2\}_2]$ (**2**), methane and ethene. The treatment of **1** with excess pinacolborane in hexane at 65 °C leads to a mixture of **2** and the paramagnetic trimer $[\{\text{Ti}(\eta^5\text{-C}_5\text{Me}_5)(\mu\text{-Cl})_2\}_3]$ (**3**). The X-ray crystal structures of compounds **2** and **3** show Ti–Ti distances of 3.267(1) and 3.219(12) Å, respectively. Computational studies (CASPT2//CASSCF and BS DFT methods) for dimer **2** reveal a singlet ground state and a relatively large singlet-triplet energy gap. Nuclear magnetic resonance (NMR) spectroscopy of **2** in aromatic hydrocarbon solutions and DFT calculations for several $[\{\text{Ti}(\eta^5\text{-C}_5\text{Me}_5)\text{Cl}_2\}_n]$ aggregates are consistent with the existence of an equilibrium between the diamagnetic dimer $[\{\text{Ti}(\eta^5\text{-C}_5\text{Me}_5)\text{Cl}(\mu\text{-Cl})_2\}_2]$ and a paramagnetic tetramer $[\{\text{Ti}(\eta^5\text{-C}_5\text{Me}_5)(\mu\text{-Cl})_2\}_4]$ in solution. In contrast, complex **2** readily dissolves in tetrahydrofuran to give a green-blue solution from which blue crystals of the mononuclear adduct $[\text{Ti}(\eta^5\text{-C}_5\text{Me}_5)\text{Cl}_2(\text{thf})]$ (**4**) were grown.

Introduction

Low-valent titanium complexes are important reagents because of their powerful reducing properties toward organic substrates and their participation in small-molecule activations. In particular, bis(cyclopentadienyl)titanium(III) chloride $[\text{Ti}(\eta^5\text{-C}_5\text{H}_5)_2\text{Cl}]$ (Nugent–RajanBabu reagent) has become increasingly popular over the last decades for promoting a broad range of organic synthetic transformations.^{1,2} The solid-state structure and magnetic properties of bis(cyclopentadienyl)titanium(III) chlorides of general formula $[\text{Ti}(\eta^5\text{-C}_5\text{H}_{5-n}\text{R}_n)_2\text{Cl}]$ are strongly influenced by the substituents on the cyclopentadienyl rings. Thus, derivatives with large R substituents on the carbon atoms of the C₅ ring are monomeric,³ while those with small R substituents are chloride-bridged dimers $[\{\text{Ti}(\eta^5\text{-C}_5\text{H}_{5-n}\text{R}_n)_2(\mu\text{-Cl})\}_2]$ according to X-ray crystal structure determinations.⁴ The monomeric species exhibit magnetic properties according to one unpaired electron per complex, but dinuclear derivatives have some degree of antiferromagnetic coupling between the two metal centers. In solution, both monomeric $[\text{Ti}(\eta^5\text{-C}_5\text{H}_{5-n}\text{R}_n)_2\text{Cl}]$ and dimeric $[\{\text{Ti}(\eta^5\text{-C}_5\text{H}_{5-n}\text{R}_n)_2(\mu\text{-Cl})\}_2]$ derivatives are in equilibrium through a half-open dimeric intermediate $[\{\text{Cl}(\eta^5\text{-C}_5\text{H}_{5-n}\text{R}_n)_2\text{Ti}\}(\mu\text{-Cl})\{\text{Ti}(\eta^5\text{-C}_5\text{H}_{5-n}\text{R}_n)_2\}]$, which appears to be the most reactive species for titanocene-mediated epoxide ring opening.⁵

By comparison, the use of monocyclopentadienyltitanium(III) halides $[\text{Ti}(\eta^5\text{-C}_5\text{R}_5)\text{X}_2]$ in organic synthesis has remained almost unexplored, although these derivatives have been known for decades.⁶ Nevertheless, half-sandwich titanium(III) species are receiving increasing attention as catalyst in organic synthesis.⁷ In particular, $[\text{Ti}(\eta^5\text{-C}_5\text{Me}_5)\text{Cl}_2]$ have been recently proposed as the active species in several radical processes although the aggregated structure of this compound remains unknown in the literature.^{7c} Historically, the first member of the halide series, $[\text{Ti}(\eta^5\text{-C}_5\text{H}_5)\text{Cl}_2]$, was prepared

accidentally by Bartlett in 1961,⁸ but the systematic studies on the syntheses and properties of these derivatives were carried out by Coutts and Wailes a few years later.⁹ The dihalide complexes were prepared by reduction of the appropriate cyclopentadienyltitanium(IV) trihalide with zinc in tetrahydrofuran and subsequent pyrolysis under high vacuum. Magnetic susceptibility measurements of $[\text{Ti}(\eta^5\text{-C}_5\text{H}_5)\text{X}_2]$ ($\text{X} = \text{Cl}, \text{Br}$) in the 100–300 K temperature range show Curie-Weiss behavior indicating some kind of association. The degree of association is unknown but dinuclear structures with two or four halide bridges have been proposed.⁶ Several reduced titanium species including $[\text{Ti}(\eta^5\text{-C}_5\text{H}_5)\text{Cl}_2]$ were also prepared by treatment of $[\text{Ti}(\eta^5\text{-C}_5\text{H}_5)\text{Cl}_3]$ with Li_3N in tetrahydrofuran.¹⁰

The analogous pentamethylcyclopentadienyl $[\text{Ti}(\eta^5\text{-C}_5\text{Me}_5)\text{Cl}_2(\text{thf})]$ and $[\text{Ti}(\eta^5\text{-C}_5\text{Me}_5)\text{Cl}_2]$ derivatives have been also prepared by conventional reduction methods of the trichloride derivative $[\text{Ti}(\eta^5\text{-C}_5\text{Me}_5)\text{Cl}_3]$. Thus, those compounds were initially isolated by Teuben and co-workers from the reaction with zinc in tetrahydrofuran, but they were only characterized by combustion analysis.¹¹ Later, Baird reported a more convenient synthesis for the dichloride complexes by reduction with manganese powder in *thf*.¹² In that study, the compounds were characterized by spectroscopic methods (UV, ^1H NMR and EPR) and were used as catalysts for the polymerization of styrene. In 2014, Mashima successfully used 1,4-bis(trimethylsilyl)-1,4-diaza-2,5-cyclohexadiene derivatives as salt-free reductants for generating a variety of low-valent early transition metal derivatives, including $[\text{Ti}(\eta^5\text{-C}_5\text{Me}_5)\text{Cl}_2]$ and $[\text{Ti}(\eta^5\text{-C}_5\text{Me}_5)\text{Cl}_2(\text{thf})]$.¹³ The crystal structure of the latter tetrahydrofuran adduct has been recently reported by Beckhaus, who obtained the crystals by reaction of $[\text{Ti}(\eta^5\text{-C}_5\text{Me}_5)\text{Cl}_3]$ with potassium diphenylphosphide in tetrahydrofuran.¹⁴

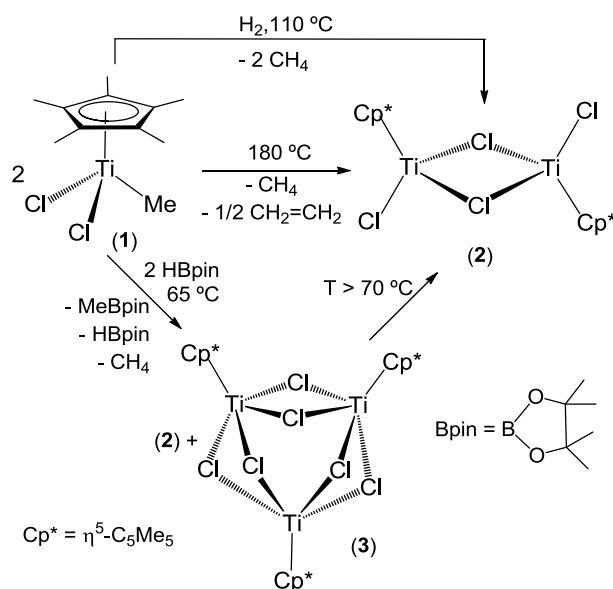
As part of a program devoted to the study of monopentamethylcyclopentadienyl titanium derivatives, we have reported that the trimethyl derivative $[\text{Ti}(\eta^5\text{-C}_5\text{Me}_5)\text{Me}_3]$ in

toluene at ≥ 95 °C gives the titanium(IV) methyldiyne cubane [$\{\text{Ti}(\eta^5\text{-C}_5\text{Me}_5)(\mu_3\text{-CH})\}_4$] and methane.¹⁵ Herein, we describe that the thermolysis of the analogous monomethyl derivative [$\text{Ti}(\eta^5\text{-C}_5\text{Me}_5)\text{Cl}_2\text{Me}$] in hydrocarbon solvents results in the clean formation of the titanium(III) dinuclear derivative [$\{\text{Ti}(\eta^5\text{-C}_5\text{Me}_5)\text{Cl}(\mu\text{-Cl})\}_2$] via elimination of methane and ethene. This salt-free route provides the dichloride complex in good yield and high purity, enabling us to undertake a detailed study of this poor-characterized titanium(III) species. The crystal structure and electronic structure of this compound and its interesting behavior in solution are discussed.

Results and Discussion

Synthesis and characterization of $[\text{Ti}(\eta^5\text{-C}_5\text{Me}_5)\text{Cl}_2]$ complexes. The treatment of $[\text{Ti}(\eta^5\text{-C}_5\text{Me}_5)\text{Cl}_3]$ with 1 equiv of trimethylaluminum $[\text{AlMe}_3]$ (2 M in toluene) in hexane at 0 °C afforded the monomethyltitanium(IV) derivative $[\text{Ti}(\eta^5\text{-C}_5\text{Me}_5)\text{Cl}_2\text{Me}]$ (**1**).¹⁶ After crystallization in hexane at –30 °C, complex **1** was isolated in good yield (60%) as orange crystals suitable for X-ray diffraction studies. The molecular structure shows the classical three-legged piano-stool arrangement for monocyclopentadienyltitanium(IV) derivatives (Figure S1 and Table S2 in the Supporting Information). The titanium–chlorine and titanium–carbon(methyl) bond lengths (2.254(1) and 2.097(2) Å, respectively) are unremarkable, and compare well with those found in the analogous complexes $[\text{Ti}(\eta^5\text{-C}_5\text{Me}_5)\text{Cl}_3]$ (av. Ti–Cl = 2.246(1) Å)¹⁷ and $[\text{Ti}(\eta^5\text{-C}_5\text{Me}_5)\text{Me}_3]$ (av. Ti–C(methyl) = 2.107(5) Å).¹⁸

Compound **1** is stable at room temperature in the solid-state and in solution under argon atmosphere. The thermal stability of **1** in benzene- d_6 was monitored by NMR spectroscopy in a flame-sealed NMR tube. At temperatures higher than 75 °C, the initial orange solution turned dark, and a new set of resonances was detected in the ^1H NMR spectrum. The complete consumption of **1** was observed after heating at 180 °C for 2 days. After that time, the spectrum at room temperature showed a broad resonance at $\delta = 6.88$ ($\Delta\nu_{1/2} = 24$ Hz) and a sharp resonance signal at $\delta = 2.09$ (*vide infra*), along with resonances assigned to methane and ethene (Scheme 1, see Figure S3 in the Supporting Information). The composition of this solution did not show any change after 24 h at room temperature according to ^1H NMR spectroscopy, but green crystals precipitated at the bottom of the tube.



Scheme 1. Synthesis of titanium(III) complexes **2** and **3**.

In a preparative scale reaction, the heating of **1** in hexane at 180 °C for 2 days afforded the precipitation of green-red crystals of the titanium(III) complex $[\{\text{Ti}(\eta^5\text{-C}_5\text{Me}_5)\text{Cl}(\mu\text{-Cl})\}_2]$ (**2**) in 90% yield. Compound **2** is highly air-sensitive in both the solid state and in solution, and quickly decomposes in air to give a mixture of products where $[\text{Ti}(\eta^5\text{-C}_5\text{Me}_5)\text{Cl}_3]$ and the dinuclear oxoderivative $[\{\text{Ti}(\eta^5\text{-C}_5\text{Me}_5)\text{Cl}_2\}_2(\mu\text{-O})]^{19}$ were identified by NMR spectroscopy. Complex **2** also reacts immediately with chloroform- d_1 to give a red solution of the trichlorotitanium(IV) derivative $[\text{Ti}(\eta^5\text{-C}_5\text{Me}_5)\text{Cl}_3]$. Similarly, addition of the stable nitroxyl radical TEMPO (2,2,6,6-tetramethylpiperidine-N-oxyl) to a solution of **2** in benzene- d_6 readily provides a red solution of the titanium(IV) complex $[\text{Ti}(\eta^5\text{-C}_5\text{Me}_5)\text{Cl}_2(\text{TEMPO})]$, as determined by ^1H and $^{13}\text{C}\{^1\text{H}\}$ NMR spectroscopy.²⁰ Nevertheless, complex **2** can be manipulated under argon atmosphere and was characterized by spectroscopic and analytical methods, as well as by an X-ray crystal structure determination. Compound **2** sublimates at 180 °C under dynamic vacuum (ca. 0.1 mmHg). Accordingly, the mass spectrum (EI, 70 eV) of **2** shows the expected molecular ion for a dimeric structure in the gas-phase, although the base peak of the spectrum

corresponds to the $[\text{Ti}(\eta^5\text{-C}_5\text{Me}_5)\text{Cl}_2]^+$ monomeric fragment. The X-ray crystal structure of **2** shows a dimer with two $[\text{Ti}(\eta^5\text{-C}_5\text{Me}_5)\text{Cl}]$ moieties held together by two bridging chloride ligands (Figure 1). The central $\text{Ti}_2(\mu\text{-Cl})_2$ core is almost planar [torsion angle $\text{Ti}(1)\text{-Cl}(3)\text{-Ti}(2)\text{-Cl}(4) = 0.97(4)^\circ$] and the $\eta^5\text{-C}_5\text{Me}_5$ ligands are arranged in a transoid fashion about that core. Each titanium atom exhibits a three-legged piano-stool geometry with one terminal chloride and two bridging chloride ligands at the legs. The titanium–chlorine bond lengths of the terminal ligands (av. $2.274(1) \text{ \AA}$) are similar to those found in complex **1**, and are clearly shorter than those associated with the bridging ligands (av. $2.392(4) \text{ \AA}$). The $\text{Ti}_2(\mu\text{-Cl})_2$ core shows Cl-Ti-Cl angles of av. $93.9(1)^\circ$ while the Ti-Cl-Ti angles (av. $86.1(1)^\circ$) are narrower.

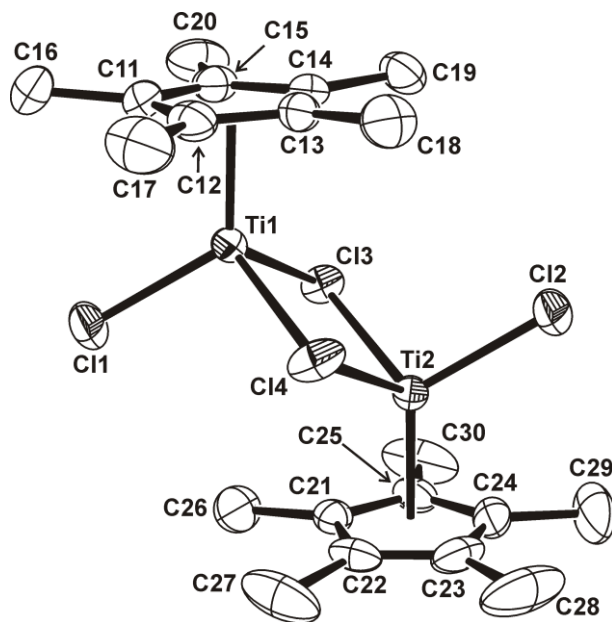


Figure 1. Perspective view of **2** with thermal ellipsoids at the 50% probability level.

Hydrogen atoms are omitted for clarity. Selected averaged lengths (\AA) and angles (deg): Ti-Ti $3.266(1)$, $\text{Ti-Cl}_{\text{terminal}}$ $2.274(1)$, $\text{Ti-Cl}_{\text{bridging}}$ $2.392(4)$, $\text{Cl}_{\text{bridging-Ti-Cl}_{\text{bridging}}}$ $93.9(1)$, $\text{Ti-Cl}_{\text{bridging-Ti}}$ $86.1(1)$.

The titanium–titanium distance in **2** of 3.266(1) Å is slightly shorter than those found in the analogous monocyclopentadienyltitanium(III) complexes [$\{\text{Ti}(\eta^5\text{-C}_5\text{Me}_4\text{Ph})\text{Cl}(\mu\text{-Cl})\}_2$] (3.335(1) Å),²¹ [$\{\text{Ti}(\eta^5\text{-C}_5(\text{CH}_2\text{Ph})_5)\text{Cl}(\mu\text{-Cl})\}_2$] (3.374(2) Å)²¹ and [$\{\text{Ti}(\eta^5\text{-C}_5\text{Me}_5)(\text{BH}_4)(\mu\text{-Cl})\}_2$] (3.452(1) Å),²² and significantly shorter than those determined in several bis(cyclopentadienyl)titanium(III) derivatives [$\{\text{Ti}(\eta^5\text{-C}_5\text{H}_5\text{-nR}_n)_2(\mu\text{-Cl})\}_2$] (3.912–4.017 Å).⁴ While the former titanium dichloride complexes were described as diamagnetic according to NMR and EPR spectroscopies in solution,²¹ [$\{\text{Ti}(\eta^5\text{-C}_5\text{Me}_5)(\text{BH}_4)(\mu\text{-Cl})\}_2$] has some paramagnetic character according to the broadened signal observed in its ¹H NMR spectrum,²² and the bis(cyclopentadienyl)titanium(III) chloride derivatives are paramagnetic compounds with an antiferromagnetic behavior which has been studied in detail in the solid-state.^{4a,9b,23,24}

Compound **2** was also prepared by reaction of [$\text{Ti}(\eta^5\text{-C}_5\text{Me}_5)\text{Cl}_3$] with Li₃N (3:1 molar ratio) or magnesium metal (2:1 molar ratio) in tetrahydrofuran and subsequent removal of the solvent under reduced pressure. However, those procedures afforded the compound contaminated by substantial amounts of the oxoderivative [$\{\text{Ti}(\eta^5\text{-C}_5\text{Me}_5)\text{Cl}_2\}_2(\mu\text{-O})$], which shows a similar solubility in organic solvents. Noteworthy, the treatment of **1** with pinacolborane (HBpin) in hydrocarbon solvents led to a mixture of the dimer **2** and the trimer [$\{\text{Ti}(\eta^5\text{-C}_5\text{Me}_5)(\mu\text{-Cl})_2\}_3$] (**3**) along with volatile by-products (Scheme 1). The reaction course of **1** with one equivalent of HBpin in benzene-d₆ was monitored by ¹H NMR spectroscopy. The spectra revealed a very slow reaction at room temperature and only after heating at 65 °C for 24 h, complete consumption of **1** was observed. The spectrum of the resultant solution shows the two resonance signals mentioned above for **2**, one broad resonance at $\delta = 8.40$ ($\Delta\nu_{1/2} = 156$ Hz) assignable to **3**, and two singlet resonances at $\delta = 0.42$ (BMe) and 1.06 (CMe) for MeBpin.²⁵ It appears that

the reaction produces a $[\text{Ti}(\eta^5\text{-C}_5\text{Me}_5)\text{Cl}_2\text{H}]$ hydride species that subsequently could release hydrogen with formation of the $[\{\text{Ti}(\eta^5\text{-C}_5\text{Me}_5)\text{Cl}_2\}_n]$ titanium(III) aggregates.²⁶ While the resonance signal for H_2 ($\delta = 4.46$) was not detected, the spectrum reveals those for methane and HBpin which could be consistent with partial hydrogenolysis of the MeBpin by-product. However, when the argon atmosphere of the NMR tube was changed by hydrogen and the tube heated at 65 °C, consumption of MeBpin was not observed. Alternatively, hydrogenolysis of part of the $[\text{Ti}(\eta^5\text{-C}_5\text{Me}_5)\text{Cl}_2\text{Me}]$ (**1**) precursor, with the H_2 generated in the reaction with HBpin, could result in $[\{\text{Ti}(\eta^5\text{-C}_5\text{Me}_5)\text{Cl}_2\}_n]$ compounds and CH_4 . Indeed, in a NMR tube experiment, exposure of a benzene- d_6 solution of **1** to 1 atm of hydrogen at 65 °C cleanly gave the resonances due to CH_4 and compound **2** in solution. Accordingly, a toluene solution of **1** under a hydrogen atmosphere at 110 °C for 3 days afforded complex **2** in 85% isolated yield (Scheme 1).

Optimization of the reaction to form compound **3** in high ratio revealed that the treatment of **1** with excess HBpin (5 equiv) at 65 °C in hexane for 7 days gave a brown solid containing a 70:30 mixture of compounds **3** and **2** by ^1H NMR spectroscopy. Compounds **2** and **3** exhibit a similar solubility in hydrocarbon solvents but crystallization in toluene at -35 °C gave a very small fraction of pure **3** as brown crystals, which were used for spectroscopic characterization and an X-ray crystal structure determination. The mass spectrum (EI, 70 eV) of **3** shows the expected molecular ion for a trimeric structure in the gas-phase, although the base peak of the spectrum corresponds to the $[\text{M-Ti}(\eta^5\text{-C}_5\text{Me}_5)\text{Cl}_3]^+$ fragment. The ^1H NMR spectrum of trimer **3** in benzene- d_6 revealed a single broad resonance at $\delta = 8.39$ ($\Delta\nu_{1/2} = 208$ Hz) for the $\eta^5\text{-C}_5\text{Me}_5$ ligands according to its paramagnetic nature. Compound **3** is stable in benzene- d_6 solution at room temperature but

readily converts into complex **2** at temperatures higher than 70 °C as determined by NMR spectroscopy.

The molecular structure of **3** reveals a trimer with three $[\text{Ti}(\eta^5\text{-C}_5\text{Me}_5)]$ moieties held together by six bridging chloride ligands (Figure 2). Each titanium atom exhibits a four-legged piano-stool geometry with four bridging chloride ligands at the legs. Thus, the titanium–chlorine bond lengths of averaged 2.443(9) Å in compound **3** are slightly longer than those found with the bridging ligands in complex **2**. The $\text{Ti}_2(\mu\text{-Cl})_2$ cores show Cl–Ti–Cl angles of 84.5(1)° and Ti–Cl–Ti angles of 82.4(3)°, which are narrower than those of complex **2**. The titanium–titanium distance in **3** of 3.219(1) Å is slightly shorter than that found in the dimer **2**. Analogous cyclic trinuclear structures have been structurally documented for complexes $[\{\text{Zr}(\eta^5\text{-1,2,4-}(t\text{Bu})_3\text{C}_5\text{H}_2)(\mu\text{-Cl})_2\}_3]^{27}$ and $[\{\text{V}(\eta^5\text{-C}_5\text{Me}_4\text{R})(\mu\text{-Cl})_2\}_3]$ (R = Me, Et).²⁸

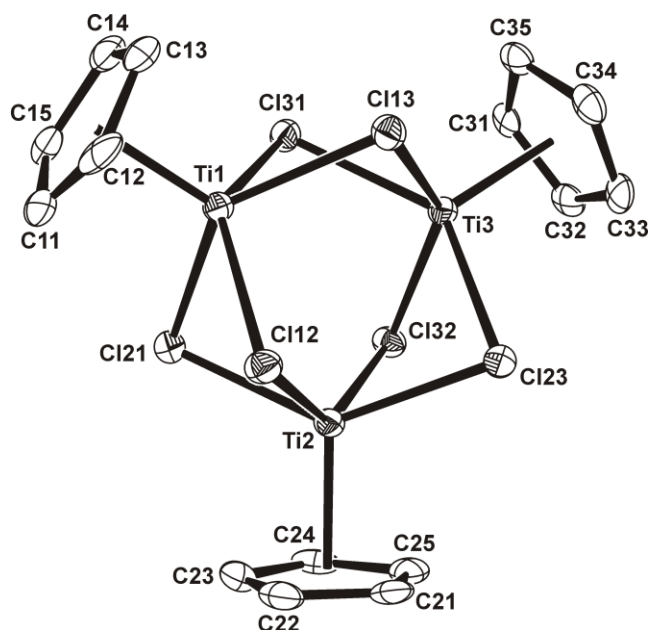


Figure 2. Perspective view of **3** with thermal ellipsoids at the 50% probability level.

Methyl groups of the pentamethylcyclopentadienyl ligands are omitted for clarity. Selected averaged lengths (Å) and angles (deg): Ti–Ti 3.219(12), Ti–Cl 2.443(9), Ti–Cl–Ti 82.4(3).

Computational Study of $[\{\text{Ti}(\eta^5\text{-C}_5\text{Me}_5)\text{Cl}(\mu\text{-Cl})\}_2]$. Theoretical calculations were conducted to establish the electronic structure and magnetic properties of the dinuclear complex **2** whose structure is shown in Figure 1. Gordon and co-workers have previously reported ab initio calculations for several homodinuclear titanium(III) molecules with bridging ligands²⁹ showing the multiconfigurational nature of the wavefunction for these species. Thus, in the current work, the first singlet and triplet states of complex **2** have been optimized using the complete active space self-consistent field (CASSCF) method.³⁰ An active space of 2 electrons in 3 orbitals was selected after benchmark (Table S8). Regarding to the singlet ground state, mainly two configurations describe this electronic state. For the first configuration the HOMO orbital is doubly occupied whereas for the second one the LUMO orbital is doubly occupied (Figure 3). Both configurations have a similar weight leading to an orbital occupation of the HOMO and LUMO orbitals of 1.06 and 0.94, respectively. In contrast to the singlet state, the triplet state is described by a single-configuration which corresponds to the monoexcitation from the HOMO to the LUMO orbital (Figure 3), leading to an occupation of 1.00 for each orbital.

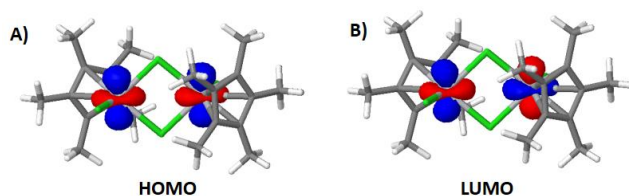


Figure 3. HOMO and LUMO involved in the singlet and triplet states of **2** computed at the CASSCF(2,3)/TZVP level.

The titanium–titanium distance of the optimized singlet ground state minimum is 3.792 Å, about 0.5 Å longer than that determined in the X-ray structure shown in Figure 1. Furthermore, this distance is even longer (3.810 Å) in the optimized first triplet state

minimum. In order to understand the failure to reproduce the intermetallic distance in the optimized structure of **2**, a scan along the Ti–Ti distance coordinate was performed at the CASSCF(2,3)/TZVP level of theory for both the singlet and the triplet state. Then, single point energy corrections have been performed at the Multi-State Complete Active Space Perturbation to the Second Order over geometries optimized at the CASSCF level (MS-CASPT2//SA-CASSCF methodology).^{30,31} The results obtained are collected in Figure 4.

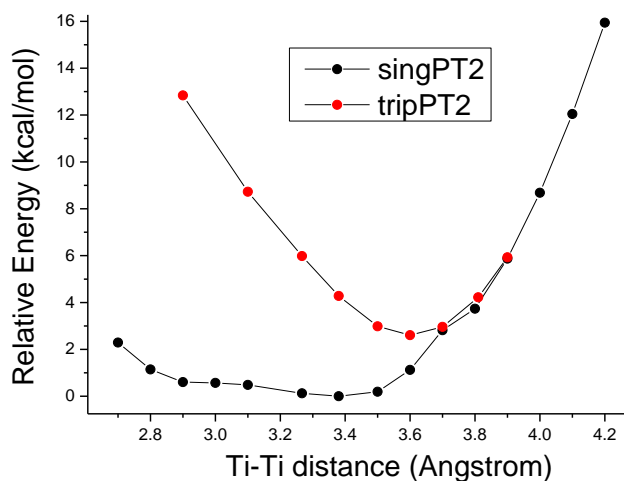


Figure 4. CASPT2//CASSCF energy corrections in the singlet and triplet states of **2** over the geometries optimized at the CASSCF level along the Ti–Ti distance.

Both the singlet and the triplet minima are slightly shifted to shorter Ti–Ti distance values when the electron dynamic correlation is considered, that is at the CASPT2//CASSCF level of theory (see Figure 4 and Table S9 in the Supporting Information). Regarding to the singlet state, the minimum is located at a titanium–titanium distance of around 3.4 Å, closer to the experimental distance experimentally measured of 3.266(1) Å (*vide supra*), than the distance found optimizing at the CASSCF level. Similarly, the Ti–Ti distance of the triplet state minimum at the CASPT2//CASSCF level is shifted up to 3.6 Å (see Figure 4).

As it can be seen in Figure 4, at the CASPT2//CASSCF level of theory, the singlet state is *ca.* 3 kcal/mol more stable than the triplet state. Likewise, the singlet-triplet energy gap is around 4 and 6 kcal/mol at the ground state minimum and at the experimental Ti–Ti distance of 3.27 Å, respectively. Noteworthy, the Ti–Ti distance can be shortened up to 2.8 Å with less than 1 kcal/mol for the singlet state whereas for the triplet state this structural deformation is energetically more demanding (~10 kcal/mol).

As aforementioned, the singlet ground state is described mainly by two configurations: the doubly-occupied HOMO and the double-occupied LUMO. In this regard, we have also analyzed how the weight of each configuration varies along the Ti–Ti distance coordinate. As expected, the shorter the distance is, the larger is the weight of the double-occupied HOMO configuration (see Table S10). This finding is in line with the larger bonding character of the HOMO orbital for the structure with the shortest Ti–Ti distance computed (Figure 5).

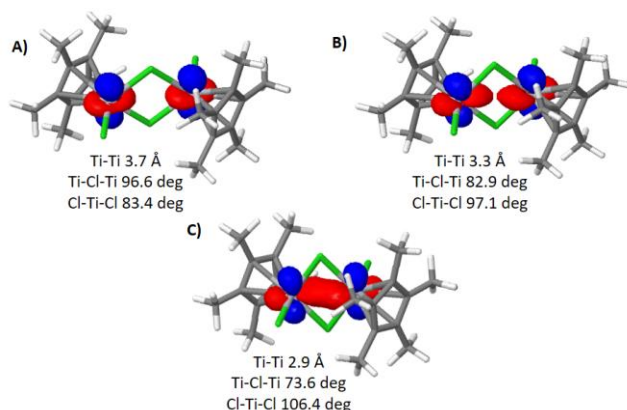


Figure 5. HOMO orbitals for **2** with Ti–Ti distances of A) 3.7, B) 3.3 and C) 2.9 Å.

Broken symmetry (BS) DFT was also used to model the multiconfigurational character of the singlet ground state of complex **2**. Single point energy calculations on the crystallographically determined atomic coordinates revealed a 3.3 kcal/mol energy difference between the singlet ground state and a triplet excited state. The closed-shell

singlet state is located at 16.0 kcal/mol above in energy that the open-shell singlet BS solution describing the ground state. Moreover, the same qualitative behavior was observed when calculations were performed on optimized geometries (see SI). Independently of the structure used in the BS DFT calculation, quite strong antiferromagnetic interaction between the metal centers was obtained as reflected by the large computed values of the coupling constant J of -1041 , -507 or -310 cm^{-1} when using the X-ray or DFT optimized structures (see Table S7). These values can be compared with that calculated for a diamagnetic dititanium(III) paddlewheel complex reported by the Cummins and Cotton groups ($J = -1266$ cm^{-1}),³² and are larger than those found in related titanocene halide complexes [$\{\text{Ti}(\eta^5\text{-C}_5\text{H}_4\text{R})_2(\mu\text{-X})\}_2$] ($X = \text{Cl}$, $R = \text{H}$, $J = -111$ cm^{-1} ; $X = \text{Cl}$, $R = \text{Me}$, $J = -160$ cm^{-1} ; $X = \text{Br}$, $R = \text{H}$, $J = -138$ cm^{-1}).^{4a} BS DFT calculations are in good agreement with CASPT2//CASSCF data presented above, supporting the singlet character of **2** and the relatively high singlet-triplet energy gap.

Solution NMR spectroscopy of $[\{\text{Ti}(\eta^5\text{-C}_5\text{Me}_5)\text{Cl}(\mu\text{-Cl})\}_2]$. The characterization of **2** by NMR spectroscopy in solution presents a puzzle and our results differ considerably from those reported previously by Baird and co-workers.¹² In that literature reference, the ^1H NMR spectra in toluene- d_8 and chlorobenzene- d_5 showed broad resonances for the $\eta^5\text{-C}_5\text{Me}_5$ ligands at $\delta = 2.10$ and 2.30 ($\Delta\nu_{1/2} = 40\text{--}80$ Hz), respectively. However, a crystallized sample of complex **2** dissolved in benzene- d_6 and the ^1H NMR spectrum at room temperature of the resultant brown solution (0.02 M) showed one broad resonance at $\delta = 6.88$ ($\Delta\nu_{1/2} = 24$ Hz) and one sharp resonance signal at $\delta = 2.09$ in a 40:60 intensity ratio.³³ The ^{13}C NMR spectrum at room temperature reveals two broad resonance signals at $\delta = 89.9$ (m) and 48.2 (q, $^1J(\text{C,H}) = 122$ Hz) and two sharp resonance signals at $\delta = 136.5$

(m) and 14.6 (q, $^1J(\text{C,H}) = 127$ Hz). The chemical shifts of the sharp resonances are in the typical range for η^5 -pentamethylcyclopentadienyl ligands of diamagnetic titanium(IV) compounds (e.g., $[\text{Ti}(\eta^5\text{-C}_5\text{Me}_5)\text{Cl}_3]$ shows $\delta_{\text{H}} = 1.87$ and $\delta_{\text{C}} = 137.4$ and 14.0 in C_6D_6). In contrast, the broad resonance at $\delta = 6.88$ ($\Delta\nu_{1/2} = 24$ Hz) found in the ^1H NMR spectrum of **2** resembles the resonance signal ($\delta = 2.58$, $\Delta\nu_{1/2} = 35$ Hz) reported for the dimeric $[\{\text{Ti}(\eta^5\text{-C}_5\text{Me}_5)(\text{BH}_4)(\mu\text{-Cl})\}_2]$ in benzene- d_6 solution.²² The quite strong antiferromagnetic interaction between the metal centers computed for complex **2** (see above) accounts for the signal at $\delta = 2.09$ found in the room temperature ^1H NMR spectrum of the complex. However, the magnetic moment measurement for a 0.01 M solution of **2** in benzene- d_6 at ambient temperature by the Evans Method³⁴ gave $\mu_{\text{eff}} = 1.37 \mu_{\text{B}}$ per dimer $[\{\text{Ti}(\eta^5\text{-C}_5\text{Me}_5)\text{Cl}(\mu\text{-Cl})\}_2]$.³⁵ This effective magnetic moment in solution at 295 K is significantly larger than that expected for the dinuclear structure and also indicates the presence of some additional paramagnetic species in solution.

Interestingly, the intensity ratio of the two resonance signals of the ^1H NMR spectrum of **2** in solution is concentration and temperature dependent. Thus, a 0.02 M solution of **2** in benzene- d_6 at room temperature showed a 40:60 intensity ratio, a 0.01 M solution revealed a 33:67 ratio, and a 0.005 M solution displayed a 27:73 ratio between the broad resonance at 6.88 ppm and the sharp resonance at 2.09 ppm. In addition, the spectrum of a 0.02 M brown solution of **2** in toluene- d_8 at 22 °C reveals one broad resonance at $\delta = 6.89$ ($\Delta\nu_{1/2} = 25$ Hz) and one sharp resonance signal at $\delta = 2.11$ in a 40:60 integration ratio. Upon heating the toluene- d_8 solution at 80 °C, the spectrum showed the broad resonance centered at $\delta = 6.20$ and the resonance signal at $\delta = 2.30$ in a 4:96 ratio. The original ratio and chemical shifts are restored on cooling the sample to room temperature.

These variations of relative intensity of the signals with temperature and concentration are consistent with a slow equilibrium in solution but the observed enhancement of the intensity of the sharp signal at high temperatures rules out the symmetric dissociation of **2** to give two paramagnetic mononuclear $[\text{Ti}(\eta^5\text{-C}_5\text{Me}_5)\text{Cl}_2]$ species. Likewise, the concentration dependence of the NMR resonances disagrees with the isomerization of **2** to yield the dinuclear $[\{\text{Ti}(\eta^5\text{-C}_5\text{Me}_5)(\mu\text{-Cl})_2\}_2]$ complex with two $[\text{Ti}(\eta^5\text{-C}_5\text{Me}_5)]$ moieties held together by four bridging chloride ligands. Alternatively, the NMR data could be consistent with the diamagnetic dimer $[\{\text{Ti}(\eta^5\text{-C}_5\text{Me}_5)\text{Cl}(\mu\text{-Cl})\}_2]$ (**2**) in equilibrium with a higher nuclearity $[\{\text{Ti}(\eta^5\text{-C}_5\text{Me}_5)\text{Cl}_2\}_n]$ ($n > 2$) species in solution (*vide infra*). However, in spite of many attempts, crystallization from benzene, toluene or hexane solutions always afforded the dimeric compound **2** and other aggregates could not be isolated and structurally characterized. As it has already been stated, the ^1H NMR spectra of a sample of independently synthesized trinuclear complex **3** presented a single broad resonance at $\delta = 8.39$ and this compound readily converts irreversibly into **2** at temperatures higher than $70\text{ }^\circ\text{C}$. Moreover, **2** and **3** are not in equilibrium in solution at room temperature, as confirmed by NMR spectroscopy. Thus, the broad resonance at $\delta = 6.88$ present in the ^1H NMR spectra of a benzene solution of **2** cannot be attributed to the presence of complex **3**.

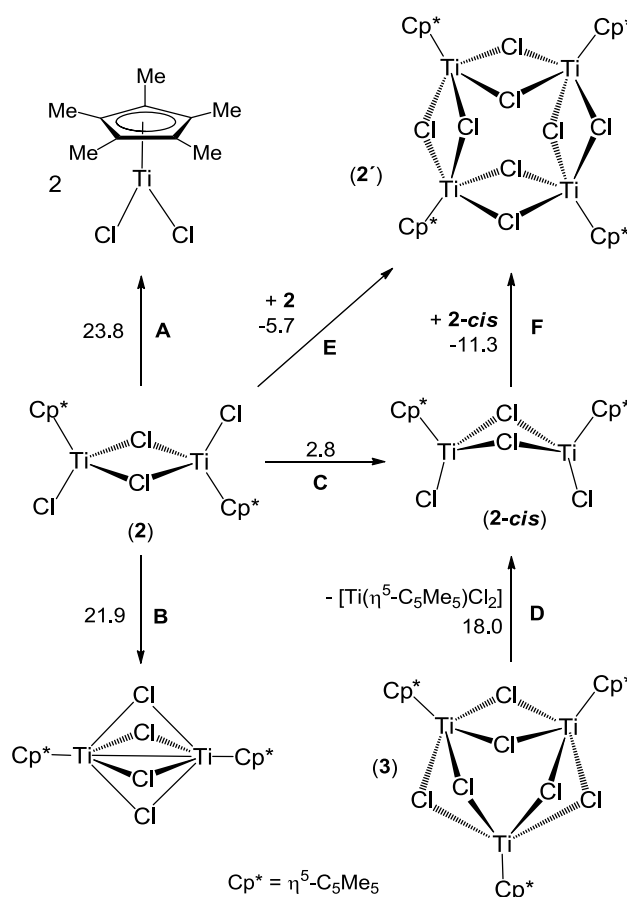
Noteworthy, addition of $[\text{Ti}(\eta^5\text{-C}_5\text{Me}_5)\text{Cl}_3]$ to a solution of **2** in benzene- d_6 does not produce any significant change in the chemical shifts and intensity ratio of the resonances due to **2** in the ^1H NMR spectrum, which also shows the resonance signal of $[\text{Ti}(\eta^5\text{-C}_5\text{Me}_5)\text{Cl}_3]$ as a sharp singlet at the expected chemical shift ($\delta = 1.87$). In contrast, the ^1H NMR spectrum recorded after addition of tetrahydrofuran to a benzene- d_6 solution of **2** showed a broadening of the resonance signal at 2.09 ppm while the resonance at 6.88 ppm

does not show any change. This is consistent with the coordination of tetrahydrofuran molecules in the dinuclear structure of **2**, which could not be possible in the locked structure of the high nuclearity aggregate. The broadening of the signal at 2.09 ppm increases with the amount of tetrahydrofuran added and, in presence of a high excess of tetrahydrofuran, this resonance virtually disappears in the spectrum. Most likely, the NMR data reported by Baird and co-workers arise from the presence of significant amounts of tetrahydrofuran in the samples of **2**, which were obtained by reduction of $[\text{Ti}(\eta^5\text{-C}_5\text{Me}_5)\text{Cl}_3]$ with manganese powder in that solvent.¹²

Compound **2** readily dissolves in tetrahydrofuran- d_8 to give a green-blue solution, and the ^1H NMR spectrum shows a single broad resonance at $\delta = 14.25$ ($\Delta\nu_{1/2} = 171$ Hz). The color change and NMR data suggest the rupture of the dinuclear structure in tetrahydrofuran to give a paramagnetic mononuclear specie. Indeed, blue crystals of the monomeric adduct $[\text{Ti}(\eta^5\text{-C}_5\text{Me}_5)\text{Cl}_2(\text{thf})]$ (**4**) were grown from a solution of **2** in tetrahydrofuran at -20 °C. Complex **4** was isolated in 50% yield and was characterized by spectroscopic and analytical methods, as well as by an X-ray crystal structure determination (Figure S2 and Table S5 in the Supporting Information). Its molecular structure is essentially the same as that found in a previous study by Beckhaus and co-workers,¹⁴ although the crystal packing is different. While the elemental analysis and the X-ray crystal structure show that in the solid-state there is one molecule of thf coordinated per titanium center in complex **4**, the analogue titanium(III) dichloride complex with the $\eta^5\text{-C}_5\text{H}_5$ ligand contains one and a half tetrahydrofuran molecules per titanium according to analytical data.^{6a} Indeed, Gambarotta and co-workers have demonstrated that $[\text{Ti}(\eta^5\text{-C}_5\text{H}_5)\text{Cl}_2(\text{thf})_{1.5}]$ crystallizes as an equimolar mixture of the four- and five-coordinate complexes $[\text{Ti}(\eta^5\text{-C}_5\text{H}_5)\text{Cl}_2(\text{thf})]$ and $[\text{Ti}(\eta^5\text{-C}_5\text{H}_5)\text{Cl}_2(\text{thf})_2]$.^{36,37} As previously observed in several studies,¹¹⁻

¹⁴ the tetrahydrofuran ligand in **4** is only weakly coordinated. Thus, once crystals of **4** are separated from the solution, the tetrahydrofuran is gradually lost within hours at room temperature to give the dinuclear compound **2**. Similarly, elimination under dynamic vacuum of the volatile components of solutions of **4** leads to a green solid characterized as **2**. Therefore, complex **4** must be stored as blue crystals under argon atmosphere at low temperatures ($-20\text{ }^{\circ}\text{C}$) or as a thf solution. The ^1H NMR spectrum of crystals of **4** in tetrahydrofuran- d_8 at room temperature reveals a single broad resonance at $\delta = 14.12$ ($\Delta\nu_{1/2} = 186\text{ Hz}$) for the $\eta^5\text{-C}_5\text{Me}_5$ ligand. The magnetic moment measurement in tetrahydrofuran- d_8 at room temperature by the Evans Method confirms its paramagnetic nature ($\mu_{\text{eff}} = 2.05\ \mu_{\text{B}}$) with one unpaired electron.³⁴

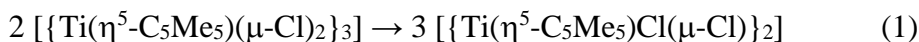
DFT Study of $[\{\text{Ti}(\eta^5\text{-C}_5\text{Me}_5)\text{Cl}_2\}_n]$ ($n = 1\text{-}4$) titanium(III) aggregates. The existence of two sets of NMR signals for benzene solutions of **2** and the variation of their relative intensity with temperature and concentration could be consistent with the presence of species of different nuclearity in solution. In this scenario, DFT calculations were performed for several $[\{\text{Ti}(\eta^5\text{-C}_5\text{Me}_5)\text{Cl}_2\}_n]$ ($n = 1\text{-}4$) titanium(III) aggregates to determine the identity of the species present in solution. Computed values of $\Delta G^0(298\text{ K})$ for several transformations among the different compounds studied are collected in Scheme 2.



Scheme 2. ΔG^0 (298 K, kcal/mol) computed values for several transformations studied.

In accord with the NMR data mentioned above, the symmetric dissociation of $[\{\text{Ti}(\eta^5\text{-C}_5\text{Me}_5)\text{Cl}(\mu\text{-Cl})\}_2]$ (**2**) to give two paramagnetic mononuclear $[\text{Ti}(\eta^5\text{-C}_5\text{Me}_5)\text{Cl}_2]$ species (reaction **A**) and the isomerization of **2** to yield the dinuclear $[\{\text{Ti}(\eta^5\text{-C}_5\text{Me}_5)(\mu\text{-Cl})_2\}_2]$ complex with four bridging chloride ligands (reaction **B**) were computed by DFT to be highly endergonic as it can be seen in Scheme 2.³⁸ In addition, the asymmetric dissociation of complex **3** yielding complex **2-cis** and the mononuclear $[\text{Ti}(\eta^5\text{-C}_5\text{Me}_5)\text{Cl}_2]$ species (reaction **D** in Scheme 2) is thermodynamically disfavored in terms of Gibbs energy, as predicted by DFT calculations, in line with the observed stability of benzene solutions of **3** at room temperature. Likewise, the conversion of complex **3** into **2** (equation

1) is computed to be slightly endergonic at 298 K ($\Delta G^0(298\text{ K}) = 6.6\text{ kcal/mol}$) and consequently higher temperatures ($> 70\text{ }^\circ\text{C}$) were experimentally needed (*vide supra*).

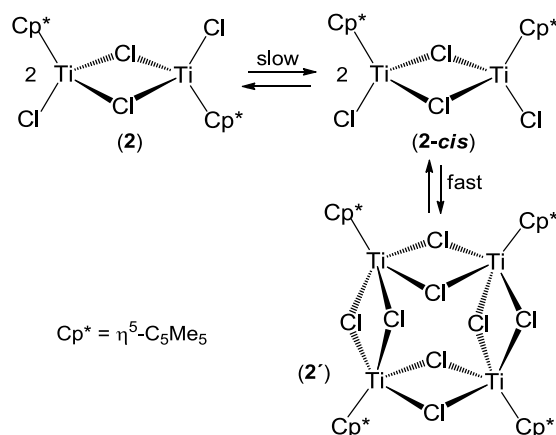


In addition to the compounds crystallographically characterized in the current work, **2** and **3**, the tetranuclear $[\{\text{Ti}(\eta^5\text{-C}_5\text{Me}_5)(\mu\text{-Cl})_2\}_4]$ (**2'**) aggregate was also calculated. The tetrameric arrangement of this species would be similar to those determined by X-ray crystallography for the analogous titanium(III) complexes $[\{\text{Ti}(\eta^5\text{-1,3-}(t\text{Bu})_2\text{C}_5\text{H}_3)(\mu\text{-F})_2\}_4]$ ³⁹ and $[\{\text{Ti}(\eta^5\text{-C}_5\text{H}_4\text{Me})(\mu\text{-Cl})(\mu\text{-OMe})\}_4]$,⁴⁰ which are paramagnetic species with μ_{eff} values of 1.74 and 1.40 μ_{B} per titanium, respectively. The two Ti...Ti distances of 3.763 and 3.777 Å in the optimized structure of $[\{\text{Ti}(\eta^5\text{-C}_5\text{Me}_5)(\mu\text{-Cl})_2\}_4]$ are in perfect agreement with that (3.772(1) Å within the $\text{Ti}_2(\mu\text{-Cl})_2$ fragment) of the crystal structure of $[\{\text{Ti}(\eta^5\text{-C}_5\text{H}_4\text{Me})(\mu\text{-Cl})(\mu\text{-OMe})\}_4]$, and are significantly longer than those observed in the molecular structures of **2** and **3** of 3.266(1) and 3.219(12) Å, respectively. The association process where two moles of **2** yield one mole of the tetranuclear derivative **2'** is thermodynamically favorable (reaction **E** in Scheme 2).

As discussed above, the $\eta^5\text{-C}_5\text{Me}_5$ ligands in the molecular structure of the dinuclear complex **2** (see Figure 1) are arranged in a transoid fashion about the central $\text{Ti}_2(\mu\text{-Cl})_2$ core and its transformation to the tetranuclear complex **2'** requires a previous isomerization of **2** to give the corresponding isomer with a cisoid arrangement about the $\text{Ti}_2(\mu\text{-Cl})_2$ moiety (**2-cis**). As it can be seen in the Supporting Information, the structural parameters of the optimized structures of both dinuclear species (**2** and **2-cis**) are quite similar (Table S6). The largest difference between them corresponds to the Ti-Cl-Ti'-Cl' torsion angle of the central $\text{Ti}_2(\mu\text{-Cl})_2$ core that increases from 0 in **2** to 25.1° in **2-cis** as a consequence of the

steric hindrance imposed by the two pentamethylcyclopentadienyl ligands located at the same side of the central $\text{Ti}_2(\mu\text{-Cl})_2$ butterfly core in the latter complex. The coupling constant computed for **2-cis** ($J = -61 \text{ cm}^{-1}$, see Supporting Information) is much less negative than that calculated for **2** and reveals a weak antiferromagnetic interaction between both titanium(III) centers. The conversion of **2** to **2-cis** is slightly endergonic (reaction **C** in Scheme 2) and present a moderate kinetic barrier ($\Delta G^\ddagger(298 \text{ K}) = 28.3 \text{ kcal/mol}$). A transition state for this isomerization was located in the triplet state⁴¹ and its molecular structure is shown in Figure S9 in the Supporting Information. Finally, a symmetric scan splitting the tetranuclear structure of **2'** to yield simultaneously two **2-cis** moieties was performed by increasing two alternate Ti···Ti distances constrained to be equal (See Figure S10). This scan reveals an almost zero activation enthalpy for the reverse reaction, the symmetric association of two dinuclear **2-cis** species to give the tetranuclear aggregate **2'**, suggesting a fast process in solution.

Based on both computational calculations and experimental evidences, we suggest that the NMR data are consistent with a diamagnetic dimer [$\{\text{Ti}(\eta^5\text{-C}_5\text{Me}_5)\text{Cl}(\mu\text{-Cl})\}_2$] (**2**) ($\delta_{\text{H}} = 2.09$) in a slow equilibrium with a paramagnetic tetramer [$\{\text{Ti}(\eta^5\text{-C}_5\text{Me}_5)(\mu\text{-Cl})_2\}_4$] (**2'**) ($\delta_{\text{H}} = 6.88$) in solution (Scheme 3).



Scheme 3. Behavior of complex **2** in solution.

In concentrations of ca. 0.02 M of **2** in C₆D₆, the ratio of dimer to tetramer is 75:25 at room temperature. In addition, based on the peak integration of the spectra at different concentrations, it is possible to conclude that when the concentration of the solution is reduced to a half of the initial (0.01 M) the symmetric dimer represents 80%, and at a concentration of 0.005 M it is 84% of the sample as expected for the associative equilibrium shown in Scheme 3. Similarly, the amount of dimer **2** in solution increases at high temperatures due to the favorable entropic term for the symmetric dissociation of the tetranuclear titanium(III) complex **2'** to yield two dinuclear [$\{\text{Ti}(\eta^5\text{-C}_5\text{Me}_5)\text{Cl}(\mu\text{-Cl})\}_2$] species.

Conclusions

The thermolysis of $[\text{Ti}(\eta^5\text{-C}_5\text{Me}_5)\text{Cl}_2\text{Me}]$ in hydrocarbon solvents results in the clean formation of the titanium(III) dimer [$\{\text{Ti}(\eta^5\text{-C}_5\text{Me}_5)\text{Cl}(\mu\text{-Cl})\}_2$] (**2**) and volatile by-products. CASPT2//CASSCF and BS DFT calculations support the singlet character of **2** and a relatively high singlet-triplet energy gap. According to NMR studies and DFT calculations, dimer **2** could establish an equilibrium in aromatic hydrocarbon solutions with a paramagnetic tetramer [$\{\text{Ti}(\eta^5\text{-C}_5\text{Me}_5)(\mu\text{-Cl})_2\}_4$]. While this tetramer could not be isolated in a pure form, an analogous trimer [$\{\text{Ti}(\eta^5\text{-C}_5\text{Me}_5)(\mu\text{-Cl})_2\}_3$] was obtained in the reaction of $[\text{Ti}(\eta^5\text{-C}_5\text{Me}_5)\text{Cl}_2\text{Me}]$ with pinacolborane. In contrast, complex **2** in tetrahydrofuran gives the paramagnetic mononuclear species $[\text{Ti}(\eta^5\text{-C}_5\text{Me}_5)\text{Cl}_2(\text{thf})]$. Based on the possibility of obtaining the half-sandwich titanium(III) dichloride complex in good yield and high purity by salt-free routes, systematic studies of the reactivity and application of this and analogous low-valent titanium species are underway in our laboratory.

Experimental Section

General Comments. All manipulations were carried out under argon atmosphere using Schlenk line or glovebox techniques. Toluene and hexane were distilled from Na/K alloy just before use. Tetrahydrofuran was distilled from purple solutions of sodium benzophenone just prior to use. NMR solvents were dried with Na (thf-d₈, toluene-d₈), Na/K alloy (C₆D₆) or calcium hydride (CDCl₃) and vacuum-distilled. Oven-dried glassware was repeatedly evacuated with a pumping system (ca. 1×10^{-3} Torr) and subsequently filled with inert gas. Thermolyses in solution at high temperatures were carried out by heating flame-sealed NMR or Carius tubes in a Roth autoclave model III. Pinacolborane (HBpin) was purchased from Aldrich and used as received. Hydrogen ($\geq 99.9999\%$, H₂O < 0.5 ppm, O₂ < 0.1 ppm) was purchased from Air Liquide and used as received. [Ti(η^5 -C₅Me₅)Cl₃]⁴² and [Ti(η^5 -C₅Me₅)Cl₂Me]¹⁶ (**1**) were prepared according to published procedures.

Samples for infrared spectroscopy were prepared as KBr pellets, and the spectra were obtained using an FT-IR Perkin-Elmer SPECTRUM 2000 or FT-IR Perkin-Elmer FRONTIER spectrophotometer. ¹H and ¹³C NMR spectra were recorded on a Varian Unity-300, Mercury-300, or Unity-500 Plus spectrometers. Chemical shifts (δ) in the ¹H and ¹³C{¹H} NMR spectra are given relative to residual protons or to carbon of the solvent, C₆D₆ (¹H: $\delta = 7.15$; ¹³C: $\delta = 128.0$), CDCl₃ (¹H: $\delta = 7.24$; ¹³C: $\delta = 77.0$) or C₄D₈O (¹H: $\delta = 3.58$; ¹³C: $\delta = 67.2$). The effective magnetic moments in solution were determined by the Evans NMR method at 295 K (using a 300 MHz instrument with a field strength of 7.05 Tesla).³⁴ Electron impact mass spectra were obtained at 70 eV on a Thermo Scientific ITQ 900 mass spectrometer. Microanalyses (C, H, N) were performed in a Heraeus CHN-O Rapid or a Leco CHNS-932 microanalyzers.

Synthesis of $[\{\text{Ti}(\eta^5\text{-C}_5\text{Me}_5)\text{Cl}(\mu\text{-Cl})\}_2]$ (2**).** *Method A:* A 100 mL Carius tube was charged with **1** (1.20 g, 4.46 mmol) and hexane (25 mL). The tube was flame-sealed and was heated at 180 °C for 2 d. The reaction mixture was allowed to cool to ambient temperature overnight to give green-red crystals and a brown solution. The Carius tube was opened in the glovebox, and the crystals were isolated by filtration onto a glass frit to afford **2** (1.02 g, 90%). *Method B:* A 150 mL ampule (Teflon stopcock) was charged with **1** (0.50 g, 1.86 mmol) and toluene (25 mL). After it was cooled at -78 °C, the argon atmosphere was changed by hydrogen. The reaction mixture was allowed to warm to room temperature and was heated at 110 °C for 3 d to give a dark brown solution. After filtration, the volatile components of the solution were removed under reduced pressure to afford **2** as a dark brown solid (0.40 g, 85%). IR (KBr, cm^{-1}): $\tilde{\nu}$ 2980 (w), 2913 (m), 1486 (w), 1425 (m), 1382 (m), 1262 (w), 1022 (m), 802 (w), 438 (vs), 367 (vs). ^1H NMR (300 MHz, C_6D_6 , 20 °C, δ): 6.88 (s br., $\Delta\nu_{1/2} = 24$ Hz; C_5Me_5), 2.09 (s; C_5Me_5). ^1H NMR ($\text{C}_6\text{D}_5\text{CD}_3$, 20 °C, δ): 6.89 (s br., $\Delta\nu_{1/2} = 25$ Hz; C_5Me_5), 2.11 (s; C_5Me_5). $^{13}\text{C}\{^1\text{H}\}$ NMR (75 MHz, C_6D_6 , 20 °C, δ): 136.5 (C_5Me_5), 90.5 (br.; C_5Me_5), 48.0 (br.; C_5Me_5), 14.5 (C_5Me_5). ^{13}C NMR (125 MHz, C_6D_6 , 20 °C, δ): 136.5 (m, C_5Me_5), 90.9 (m br.; C_5Me_5), 48.3 (q, $^1J(\text{C},\text{H}) = 122$ Hz; C_5Me_5), 14.6 (q, $^1J(\text{C},\text{H}) = 127$ Hz; C_5Me_5). MS (EI, 70 eV): m/z (%): 508 (29) $[\text{M}]^+$, 253 (100) $[\text{Ti}(\text{C}_5\text{Me}_5)\text{Cl}_2]^+$, 217 (61) $[\text{Ti}(\text{C}_5\text{Me}_5)\text{Cl}]^+$. Anal. Calcd. for $\text{C}_{20}\text{H}_{30}\text{Cl}_4\text{Ti}_2$ ($M_w = 508.03$): C 47.28, H 5.95. Found: C 47.19, H 5.84. The effective magnetic moment of **2** was determined to be 1.37 μ_B (based on a unit formula of $\text{C}_{20}\text{H}_{30}\text{Cl}_4\text{Ti}_2$) on a C_6D_6 solution.

Reaction of **1 with excess HBpin.** A 50 mL ampule (Teflon stopcock) was charged with **1** (0.30 g, 1.11 mmol), HBpin (0.70 g, 5.57 mmol), and hexane (20 mL). The reaction mixture was heated at 65 °C for 7 days to give a dark brown precipitate and a brown solution. The solid (0.18 g) was isolated by filtration onto a glass frit and its ^1H NMR

spectrum in benzene- d_6 revealed a 70 and 30% mixture of complexes [$\{\text{Ti}(\eta^5\text{-C}_5\text{Me}_5)(\mu\text{-Cl})_2\}_3$] (**3**) and **2**, respectively. This solid was dissolved in toluene (3 mL) and the resultant solution was cooled to $-35\text{ }^\circ\text{C}$ for 1 month to afford brown crystals of **3** (0.005 g, 2%). An additional crop of crystals could be obtained by concentration and cooling of the resultant solution, although the ^1H NMR spectra showed it to be a mixture of compounds **2** and **3**.

Spectroscopic data for **3**: IR (KBr, cm^{-1}): $\tilde{\nu}$ 2976 (m), 2964 (m), 2905 (s), 2852 (m), 1488 (m), 1453 (m), 1429 (s), 1375 (vs), 1262 (m), 1100 (w), 1021 (s), 802 (s), 402 (s). ^1H NMR (300 MHz, C_6D_6 , $20\text{ }^\circ\text{C}$, δ): 8.40 (s br., $\Delta\nu_{1/2} = 156\text{ Hz}$; C_5Me_5). MS (EI, 70 eV): m/z (%): 762 (21) $[\text{M}]^+$, 726 (2) $[\text{M-Cl}]^+$, 508 (76) $[\text{M-Ti}(\text{C}_5\text{Me}_5)\text{Cl}_2]^+$, 472 (100) $[\text{M-Ti}(\text{C}_5\text{Me}_5)\text{Cl}_3]^+$, 253 (34) $[\text{Ti}(\text{C}_5\text{Me}_5)\text{Cl}_2]^+$, 218 (79) $[\text{Ti}(\text{C}_5\text{Me}_5)\text{Cl}]^+$.

Synthesis of $[\text{Ti}(\eta^5\text{-C}_5\text{Me}_5)\text{Cl}_2(\text{thf})]$ (4**).** A 25 mL Schlenk tube was charged with **2** (0.20 g, 0.39 mmol) and tetrahydrofuran (5 mL). The resultant green-blue solution was filtered, concentrated under reduced pressure to ca. 1-2 mL, and allowed to crystallize at $-20\text{ }^\circ\text{C}$ for 4 days. After decantation, the resultant blue crystals were allowed to dry for 15 min at room temperature and were characterized as **4** (0.13 g, 50%). Crystals of **4** must be stored at low temperature in order to prevent loss of tetrahydrofuran. IR (KBr, cm^{-1}): $\tilde{\nu}$ 3327 (w), 2977 (s), 2913 (s), 1602 (w), 1487 (m), 1427 (m), 1378 (s), 1262 (w), 1343 (w), 1248 (w), 1175 (w), 1067 (w), 1022 (w), 1009 (vs), 954 (w), 919 (m), 858 (vs), 802 (w), 761 (m), 683 (w), 619 (w), 436 (vs). ^1H NMR (300 MHz, $\text{C}_4\text{D}_8\text{O}$, $20\text{ }^\circ\text{C}$, δ): 14.12 (s br., $\Delta\nu_{1/2} = 186\text{ Hz}$; C_5Me_5). Anal. Calcd for $\text{C}_{14}\text{H}_{23}\text{Cl}_2\text{OTi}$ ($M_w = 326.11$): C 51.56, H 7.11. Found: C 51.72, H 6.45. The effective magnetic moment of **4** was determined to be $2.05\ \mu_B$ (based on a unit formula of $\text{C}_{14}\text{H}_{23}\text{Cl}_2\text{OTi}$) on a $\text{C}_4\text{D}_8\text{O}$ solution.

X-ray crystal structure determinations. Orange crystals of **1** were obtained from a hexane solution at $-30\text{ }^\circ\text{C}$. Green-red crystals of compound **2**, green crystals of **3**, and blue

crystals of **4** were obtained as described in the Experimental Section. The crystals were removed from the Schlenk and covered with a layer of a viscous perfluoropolyether (FomblinY). A suitable crystal was selected with the aid of a microscope, mounted on a cryoloop, and immediately placed in the low temperature nitrogen stream of the diffractometer. The intensity data sets were collected at 150 or 200 K on a Bruker-Nonius KappaCCD diffractometer equipped with an Oxford Cryostream 700 unit. Crystallographic data for all the complexes are presented in Table S1 of the Supporting Information.

The structures were solved, using the WINGX package,⁴³ by intrinsic phasing methods (SHELXT),⁴⁴ and refined by least-squares against F^2 (SHELXL-2014/7).⁴⁵ In the crystallographic study of complexes **1**, **2**, **3**, and **4** all non-hydrogen atoms were anisotropically refined, whereas all hydrogen atoms were included, positioned geometrically and refined by using a riding model. Additionally, for **2** DELU restraints were applied for the carbon atoms C(24) and C(29).

Computational Details. The relative stability of several oligomers of $[\text{Ti}(\eta^5\text{-C}_5\text{Me}_5)\text{Cl}_2]$ was computationally evaluated. The geometries of the different species were optimized at the DFT level of theory using the PBE0⁴⁶ functional, the D3(BJ) empirical dispersion correction⁴⁷ and def2-SV(P)⁴⁸ basis set. To further refine the energies obtained from the PBE0-D3(BJ)/def2-SV(P) calculations, single-point calculations on the previously optimized structures were finally performed using the larger def2-TZVP basis set.

For predicting exchange coupling constants J we employed the broken symmetry (BS) methodology⁴⁹ using the approach proposed by Yamaguchi and co-workers⁵⁰ (see Supporting Information). When possible, the X-ray structure was used. Otherwise, the structure was optimized at the DFT level of theory with the B3LYP-D3(BJ)^{47,51} functional and def2-SV(P)⁴⁸ basis set. In both cases, the energies were computed with the larger def2-TZVP basis set.

Due to the known multiconfigurational nature of the wavefunction of some dinuclear Ti complexes,²⁹ the complete active space self-consistent field (CASSCF)³⁰ method was also used for the study of the electronic structure and the relative energy of the singlet and triplet states of the dimer [$\{\text{Ti}(\eta^5\text{-C}_5\text{Me}_5)\text{Cl}(\mu\text{-Cl})\}_2$]. The TZVP basis set was selected as well as the active space of 2 electrons in 3 orbitals. This basis set and active space were selected after performing a benchmark (see Supporting Information). Single point energy corrections were performed at the Multi-State Complete Active Space Perturbation to the Second Order (MS-CASPT2//SA-CASSCF methodology).³¹

All calculations were performed with the Gaussian 16⁵² suit of program except the CASPT2//CASSCF calculations that were done with Open Molcas.⁵³

Associated Content:

Supporting Information.

The Supporting Information is available free of charge on the ACS Publications website at DOI: 10.2021/acs.inorg-chem.xxxxxx.

Experimental crystallographic data of complexes **1-4**; perspective views of the crystal structure of complexes **1** and **4**; tables for selected lengths and angles of the crystal structures of **1-4**; ¹H NMR spectra of the thermolysis of **1**; selected NMR spectra of compounds **2-4**; full description of computational methods and Cartesian coordinates of the optimized complexes (PDF).

Accession Codes:

CCDC 1895482-1895485 contain the supplementary crystallographic data for this paper. These data can be obtained free of charge via www.ccdc.ac.uk/data_request/cif, or by emailing data_request@ccdc.cam.ac.uk, or by contacting The Cambridge

Crystallographic Data Centre, 12 Union Road, Cambridge CB2 1EZ, UK; fax: +44 1223 336033.

Author Information

Corresponding Authors

*E-mail: manuel.temprado@uah.es

*E-mail: carlos.yelamos@uah.es

ORCID

Cristina García-Iriepa: 0000-0002-7577-8242

Estefanía del Horno: 0000-0001-8900-4371

Avelino Martín: 0000-0002-9776-9670

Miguel Mena: 0000-0001-7456-1212

Adrián Pérez-Redondo: 0000-0002-0086-8825

Manuel Temprado: 0000-0002-2003-4588

Carlos Yélamos: 0000-0003-0425-4799

Notes

The authors declare no competing financial interest.

Acknowledgments

We thank Diego Sampedro of the Universidad de la Rioja for technical assistance with DFT calculations. We are also grateful to Spanish MINECO (CTQ2013-44625-R and CTQ2016-80600-P), and Universidad de Alcalá (CCG2017-EXP/021) for financial support of this research. E.H. thanks the Universidad de Alcalá for a fellowship.

References

-
- (1) For pioneering reports on the use of this reagent, see: (a) Nugent, W. A.; RajanBabu, T. V. Transition-Metal-Centered Radicals in Organic Synthesis. Titanium(III)-Induced Cyclization of Epoxy Olefins. *J. Am. Chem. Soc.* **1988**, *110*, 8561–8562. (b) RajanBabu, T. V.; Nugent, W. A. Intermolecular Addition of Epoxides to Activated Olefins: a New Reaction. *J. Am. Chem. Soc.* **1989**, *111*, 4525–4527. (c) RajanBabu, T. V.; Nugent, W. A.; Beattie, M. S. Free Radical-Mediated Reduction and Deoxygenation of Epoxides. *J. Am. Chem. Soc.* **1990**, *112*, 6408–6409. (d) RajanBabu, T. V.; Nugent, W. A. Selective Generation of Free Radicals from Epoxides Using a Transition-Metal Radical. A Powerful New Tool for Organic Synthesis. *J. Am. Chem. Soc.* **1994**, *116*, 986–997.
- (2) For reviews on the use of this reagent, see: (a) Gansäuer, A.; Bluhm, H. Reagent-Controlled Transition-Metal-Catalyzed Radical Reactions. *Chem. Rev.* **2000**, *100*, 2771–2788. (b) Barrero, A. F.; Quílez del Moral, J. F.; Sánchez, E. M.; Arteaga, J. F. Titanocene-Mediated Radical Cyclization: An Emergent Method Towards the Synthesis of Natural Products. *Eur. J. Org. Chem.* **2006**, 1627–1641. (c) Gansäuer, A.; Justicia, J.; Fan, C.-A.; Worgull, D.; Piestert, F. Reductive C–C Bond Formation after Epoxide Opening via Electron Transfer. In (Krische M. J. Ed) Metal Catalyzed Reductive C–C Bond Formation. *Topics in Current Chemistry*, Vol. 279, Springer: Berlin, **2007**, 25–52. (d) Morcillo, S. P.; Miguel, D.; Campaña, A. G.; Álvarez de Cienfuegos, L.; Justicia, J.; Cuerva, J. M. Recent Applications of Cp₂TiCl in Natural Product Synthesis. *Org. Chem. Front.* **2014**, *1*, 15–33. (e) Castro-Rodríguez, M.; Rodríguez-García, I.; Rodríguez-Maecker, R. N.; Pozo-Morales, L.; Oltra J. E.; Rosales-Martínez, A. Cp₂TiCl: An Ideal Reagent for Green Chemistry? *Org. Process Res. Dev.* **2017**, *21*, 911–923. (f) Botubol-Ares, J. M.; Durán-Peña, M. J.; Hanson, J. R.;

Hernández-Galán, R.; Collado, I. G. Cp₂Ti(III)Cl and Analogues as Sustainable Templates in Organic Synthesis. *Synthesis* **2018**, *50*, 2163–2180.

- (3) (a) Pattiasina, J. W.; Heeres, H. J.; van Bolhuis, F.; Meetsma, A.; Teuben, J. H.; Spek, A. L. Monomeric Bis(pentamethylcyclopentadienyl)titanium(III) Complexes with Halide, Borohydride, Amide, Alkoxide, and Carboxylate Ligands. X-ray Structure of Bis(pentamethylcyclopentadienyl)titanium(III) Chloride. *Organometallics* **1987**, *6*, 1004–1010. (b) Troyanov, S. I.; Rybakov, V. B.; Thewalt, U.; Varga, V.; Mach, K. Crystal and Molecular Structure of Bis(tetramethylcyclopentadienyl)titanium Halides, (C₅HMe₄)₂TiCl, (C₅HMe₄)₂TiI and (C₅HMe₄)₂TiCl₂. *J. Organomet. Chem.* **1993**, *447*, 221–225. (c) Walter, M. D.; Sofield, C. D.; Andersen, R. A. Preparation and Reactions of Base-Free Bis(1,3-*tert*-butylcyclopentadienyl)titanium, Cp'₂Ti, and Related Compounds. *Organometallics* **2008**, *27*, 2959–2970.
- (4) (a) Jungst, R.; Sekutowski, D.; Davis, J.; Luly, M.; Stucky, G. D. Structural and Magnetic Properties of Di-μ-chloro-bis[bis(η⁵-cyclopentadienyl)titanium(III)] and Di-μ-bromo-bis[bis(η⁵-methylcyclopentadienyl)titanium(III)]. *Inorg. Chem.* **1977**, *16*, 1645–1655. (b) Mach, K.; Varga, V.; Schmid, G.; Hiller, J.; Thewalt, U. The Dimeric Structure of Bis(1,3-Dimethylcyclopentadienyl)titanium(III) Chloride. *Collect. Czech. Chem. Commun.* **1996**, *61*, 1285–1294. (c) Klahn, M.; Arndt, P.; Spannenberg, A.; Gansäuer, A.; Rosenthal, U. Menthyl-Substituted Group 4 Metallocene Dihalides. *Organometallics* **2008**, *27*, 5846–5851. (d) Krizan, M.; Honzicek, J.; Vinklerek, J.; Ruzickova, Z.; Erben, M. Titanocene(III) Pseudohalides: An ESR and Structural Study. *New J. Chem.* **2015**, *39*, 576–588.
- (5) (a) Daasbjerg, K.; Svith, H.; Grimme, S.; Gerenkamp, M.; Mück-Lichtenfeld, C.; Gansäuer, A.; Barchuk, A.; Keller, F. Elucidation of the Mechanism of Titanocene-Mediated Epoxide Opening by a Combined Experimental and Theoretical Approach.

-
- Angew. Chem. Int. Ed.* **2006**, *45*, 2041–2044. (b) Gansäuer, A.; Barchuk, A.; Keller, F.; Schmitt, M.; Grimme, S.; Gerenkamp, M.; Mück-Lichtenfeld, C.; Daasbjerg, K.; Svith, H. Mechanism of Titanocene-Mediated Epoxide Opening through Homolytic Substitution. *J. Am. Chem. Soc.* **2007**, *129*, 1359–1371.
- (6) (a) Wailes, P. C.; Coutts, R. S. P.; Weigold, H. *Organometallic Chemistry of Titanium, Zirconium and Hafnium*; Academic Press: New York, 1974. (b) Poli, R. Monocyclopentadienyl Halide Complexes of the d- and f-Block Elements. *Chem. Rev.* **1991**, *91*, 509–551.
- (7) (a) Hao, W.; Wu, X.; Sun, J. Z.; Siu, J. C.; MacMillan, S. N.; Lin, S. Radical Redox-Relay Catalysis: Formal [3+2] Cycloaddition of N-Acylaziridines and Alkenes. *J. Am. Chem. Soc.* **2017**, *139*, 12141–12144. (b) Hao, W.; Harenberg, J. H.; Wu, X.; MacMillan, S. N.; Lin, S. Diastereo- and Enantioselective Formal [3+2] Cycloaddition of Cyclopropyl Ketones and Alkenes via Ti-Catalyzed Radical Redox-Relay. *J. Am. Chem. Soc.* **2018**, *140*, 3514–3517. (c) Wu, X.; Hao, W.; Ye, K.-Y.; Jiang, B.; Pombar, G.; Song, Z.; Lin, S. Ti-Catalyzed Radical Alkylation of Secondary and Tertiary Alkyl Chlorides Using Michael Acceptors. *J. Am. Chem. Soc.* **2018**, *140*, 14836–14843. (d) Okamoto, S.; Yamada, T.; Tanabe, Y.; Sakai, M. Alkyne [2 + 2 + 2] Cyclootrimerization Catalyzed by a Low-Valent Titanium Reagent Derived from CpTiX₃ (X = Cl, O-*i*-Pr), Me₃SiCl, and Mg or Zn. *Organometallics* **2018**, *37*, 4431–4438; and references therein.
- (8) Bartlett, P. D.; Seidel, B. Monocyclopentadienyltitanium Dichloride. *J. Am. Chem. Soc.* **1961**, *83*, 581–584.
- (9) (a) Canty, A. J.; Coutts, R. S. P.; Wailes, P. C. The Magnetic Properties of the Cyclopentadienyltitanium(III) Derivatives, cpTiCl₂, cp₂TiCl, and cp₃Ti. *Aust. J. Chem.* **1968**, *21*, 807–810. (b) Coutts, R. S. P.; Martin, R. L.; Wailes, P. C.

-
- Monocyclopentadienyltitanium(III) Compounds. *Aust. J. Chem.* **1971**, *24*, 1079–1080. (c) Coutts, R. S. P.; Martin, R. L.; Wailes, P. C. Monocyclopentadienyltitanium(III) Compounds I. Halides and Their Tetrahydrofuran Complexes. *Aust. J. Chem.* **1971**, *24*, 2533–2540.
- (10) (a) Kilner, M.; Parkin, G.; Talbot, A. G. Synthetic Use of Lithium Nitride, an Unusual Reducing Agent. Formation of Ti_4 and Ti_6 Complexes. *J. Chem. Soc., Chem. Commun.* **1985**, 34–35. (b) Kilner, M.; Parkin, G. Lithium Nitride Reduction of Cp_2TiCl_2 and $CpTiCl_3$: The Synthesis of $(Cp_2TiCl)_2$, $(CpTiCl)_n$, $Cp_2Ti(CO)_2$ and Chlorotetratitanium and Nitridohexatitanium Complexes. *J. Organomet. Chem.* **1986**, *302*, 181–191.
- (11) Nieman, J.; Pattiasina, J. W.; Teuben, J. H. Synthesis and Characterization of Bis-Benzyl and Bis-Allyl Complexes of Titanium(III) and Vanadium(III); Catalytic Isomerization of Alkenes with $CpV(\eta^3-C_3H_5)_2$. *J. Organomet. Chem.* **1984**, *262*, 157–169.
- (12) Williams, E. F.; Murray, M. C.; Baird, M. C. Oxidation State(s) of the Active Titanium Species during Polymerization of Styrene to Syndiotactic Polystyrene Catalyzed by $Cp^*TiMe_3/B(C_6F_5)_3$, $Cp^*TiMe_3/[Ph_3C][B(C_6F_5)_4]$, and $Cp^*TiCl_{2,3}/MAO$. *Macromolecules* **2000**, *33*, 261–268.
- (13) Saito, T.; Nishiyama, H.; Tanahashi, H.; Kawakita, K.; Tsurugi, H.; Mashima, K. 1,4-Bis(trimethylsilyl)-1,4-diaza-2,5-cyclohexadienes as Strong Salt-Free Reductants for Generating Low-Valent Early Transition Metals with Electron-Donating Ligands. *J. Am. Chem. Soc.* **2014**, *136*, 5161–5170.
- (14) Oswald, T.; Schmidtman, M.; Beckhaus, R. Crystal Structure of $(\eta^5$ -pentamethylcyclopentadienyl)titanium(III)dichloride (THF), $C_{14}H_{23}Cl_2OTi$. *Z. Kristallogr. NCS* **2016**, *231*, 637–639.

-
- (15) Andrés, R.; Gómez-Sal, P.; de Jesús, E.; Martín, A.; Mena, M.; Yélamos, C. Thermal Decomposition of $[(\eta^5\text{-C}_5\text{Me}_5)\text{TiMe}_3]$: Synthesis and Structure of the Methyldiyne Cubane $[(\eta^5\text{-C}_5\text{Me}_5)\text{Ti}]_4(\mu_3\text{-CH})_4$. *Angew. Chem. Int. Ed. Engl.* **1997**, *36*, 115–117.
- (16) Martín, A.; Mena, M.; Pellinghelli, M. A.; Royo, P.; Serrano, R.; Tiripichio, A. Some Insertion Reactions into the Ti–Me Bond of $[\text{Ti}(\eta^5\text{-C}_5\text{Me}_5)\text{MeCl}_2]$; Crystal Structures of $[\text{Ti}(\eta^5\text{-C}_5\text{Me}_5)(\eta^2\text{-COMe})\text{Cl}_2]$ and $[\{\text{Ti}(\eta^5\text{-C}_5\text{Me}_5)\}_2(\mu\text{-Cl})_2\{\mu\text{-}\eta^4\text{-CH}_2\text{-}(2,6\text{-Me}_2\text{C}_6\text{H}_3\text{N})\text{C}=\text{C}(\text{NC}_6\text{H}_3\text{Me}_{2-2,6})\text{CH}_2\}]$. *J. Chem. Soc., Dalton Trans.* **1993**, 2117–2122.
- (17) Pevec, A. Crystal Structures of $(\eta^5\text{-C}_5\text{Me}_5)\text{TiCl}_3$ and $(\eta^5\text{-C}_5\text{Me}_4\text{H})\text{TiCl}_3$. *Acta Chim. Slov.* **2003**, *50*, 199–206.
- (18) Blom, R.; Rypdal, K.; Mena, M.; Royo, P.; Serrano, R. The Molecular Structure of Me_3TiCp^* in the Gas Phase. *J. Organomet. Chem.* **1990**, *391*, 47–51.
- (19) Palacios, F.; Royo, P.; Serrano, R.; Balcázar, J. L.; Fonseca, I.; Florencio, F. The Hydrolysis of Pentamethylcyclopentadienyltitanium Trihalides and the Formation of Di-, Tri-, and Tetra-Nuclear μ -Oxo Complexes. Crystal Structure of $[(\text{C}_5\text{Me}_5)\text{TiBr}(\mu\text{-O})]_4\text{CHCl}_3$, which Contains a Ti_4O_4 Ring. *J. Organomet. Chem.* **1989**, *375*, 51–58.
- (20) Mahanthappa, M. K.; Cole, A. P.; Waymouth, R. M. Synthesis, Structure, and Ethylene/ α -Olefin Polymerization Behavior of (Cyclopentadienyl)(nitroxide)titanium Complexes. *Organometallics* **2004**, *23*, 836–845.
- (21) Schmid, G.; Thewalt, U.; Sedmera, P.; Hanus, V.; Mach, K. Dimeric Structures of Cp^*TiCl_2 Compounds with Bulky Substituents at the Cyclopentadienyl Rings. *Collect. Czech. Chem. Commun.* **1998**, *63*, 636–645.
- (22) Kim, D. Y.; You, Y.; Girolami, G. S. Synthesis and Crystal Structure of Two (Cyclopentadienyl)titanium(III) Hydroborate Complexes, $[\text{Cp}^*\text{TiCl}(\text{BH}_4)]_2$ and $\text{Cp}_2\text{Ti}(\text{B}_3\text{H}_8)$. *J. Organomet. Chem.* **2008**, *693*, 981–986.

-
- (23) (a) Martin, R. L.; Winter, G. The Metal-Metal Bond in Binuclear Di- π -cyclopentadienyltitanium(III) Chloride. *J. Chem. Soc.* **1965**, 4709–4714. (b) Coutts, R. S. P.; Wailes, P. C.; Martin, R. L. Dimeric Dicyclopentadienyltitanium(III) Halides. *J. Organomet. Chem.* **1973**, *47*, 375–382.
- (24) Enders, M.; Fink, J.; Maillant, V.; Pritzkow, H. Synthesis, Structure, and Reactivity of Metal Complexes with Alkoxydimethyl Ligands. *Z. Anorg. Allg. Chem.* **2001**, *627*, 2281–2288.
- (25) (a) Brown, H. C.; Park, W. S.; Cha, J. S.; Cho, B. T.; Brown, C. A. Addition Compounds of Alkali Metal Hydrides. 28. Preparation of Potassium Dialkoxymonoalkylborohydrides from Cyclic Boronic Esters. A New Class of Reducing Agents. *J. Org. Chem.* **1986**, *51*, 337–342. (b) Pécharman, A.-F.; Colebatch, A. L.; Hill, M. S.; McMullin, C. L.; Mahon, M. F.; Weetman, C. Easy Access to Nucleophilic Boron through Diborane to Magnesium Boryl Metathesis. *Nat. Commun.* **2017**, *8*, 15022.
- (26) A recent article has demonstrated that the related hydride chloride $[\text{Ti}(\eta^5\text{-C}_5\text{H}_5)_2\text{ClH}]$ species is thermally unstable and undergoes intermolecular reductive elimination of molecular hydrogen to generate $[\text{Ti}(\eta^5\text{-C}_5\text{H}_5)_2\text{Cl}]$, see: Gordon, J.; Hildebrandt, S.; Dewese, K. R.; Klare, S.; Gansäuer, A.; RajanBabu, T. V.; Nugent, W. A. Demystifying $\text{Cp}_2\text{Ti}(\text{H})\text{Cl}$ and Its Enigmatic Role in the Reactions of Epoxides with Cp_2TiCl . *Organometallics* **2018**, *37*, 4801–4809.
- (27) Schäfer, S.; Bauer, H.; Becker, J.; Sun, Y.; Sitzmann, H. Cyclononatetraenyl-Indenyl Transformations and a Zirconium(III) Trimer from Bulky Alkylcyclopentadienylzirconium Chlorides. *Eur. J. Inorg. Chem.* **2013**, 5694–5700.
- (28) (a) Ting, C.; Hammer, M. S.; Baenziger, N. C.; Messerle, L.; Deak, J.; Li, S.; McElfresh, M. Dimeric and Cyclotrimeric Piano-Stool Vanadium(III) Dihalides with Unusual

-
- Differences in V–V Distance and Magnetochemistry. Syntheses, Structures, and Reactivities of $(\eta\text{-C}_5\text{Me}_4\text{R})_2\text{V}_2(\mu\text{-Br})_4$ and the Trivanadium Cluster $(\eta\text{-C}_5\text{Me}_4\text{R})_3\text{V}_3(\mu\text{-Cl})_6$, New Mid-Valent Organovanadium Synthons. *Organometallics* **1997**, *16*, 1816–1818. (b) Abernethy, C. D.; Bottomley, F.; Decken, A.; Thompson, R. C. Organometallic Halides: Preparation and Physical and Chemical Properties of Tris[(η -pentamethylcyclopentadienyl)dichlorovanadium], $[(\eta\text{-C}_5\text{Me}_5)\text{V}(\mu\text{-Cl})_2]_3$. *Organometallics* **1997**, *16*, 1865–1869.
- (29) (a) Webb, S. P.; Gordon, M. S. Molecular Electronic Structure and Energetics of the Isomers of Ti_2H_6 . *J. Am. Chem. Soc.* **1998**, *120*, 3846–3857. (b) Aikens, C. M.; Gordon, M. S. Electronic Structure and Magnetic Properties of $\text{Y}_2\text{Ti}(\mu\text{-X})_2\text{TiY}_2$ (X, Y = H, F, Cl, Br) Isomers. *J. Phys. Chem. A* **2003**, *107*, 104–114. (c) Aikens, C. M.; Gordon, M. S. Influence of Multi-atom Bridging Ligands on the Electronic Structure and Magnetic Properties of Homodinuclear Titanium Molecules. *J. Phys. Chem. A* **2005**, *109*, 11885–11901.
- (30) Roos, B. O.; Taylor, P. R.; Siegbahn, P. E. M. A Complete Active Space SCF Method (CASSCF) Using a Density Matrix Formulated Super-CI Approach. *Chem. Phys.* **1980**, *48*, 157–173.
- (31) Finley, J.; Malmqvist, P. Å.; Roos, B. O.; Serrano-Andrés, L. The Multi-State CASPT2 Method. *Chem. Phys. Lett.* **1998**, *288*, 299–306.
- (32) Mendiratta, A.; Cummins, C. C.; Cotton, F. A.; Ibragimov, S. A.; Murillo, C. A.; Villagrán, D. A Diamagnetic Ditungsten(III) Paddlewheel Complex with No Direct Metal–Metal Bond. *Inorg. Chem.* **2006**, *45*, 4328–4330.
- (33) Identical resonance signals have been found in the spectra of powdered samples of complex **2** prepared by treatment of $[\text{Ti}(\eta^5\text{-C}_5\text{Me}_5)\text{Cl}_3]$ with conventional reducing agents (Li_3N , Mg).

-
- (34) (a) Evans, D. F. The Determination of the Paramagnetic Susceptibility of Substances in Solution by Nuclear Magnetic Resonance. *J. Chem. Soc.* **1959**, 2003–2005. (b) Sur, S. K. Measurement of Magnetic Susceptibility and Magnetic Moment of Paramagnetic Molecules in Solution by High-Field Fourier Transform NMR Spectroscopy. *J. Magn. Reson.* **1989**, 169–173. (c) Bain, G. A.; Berry, J. F. Diamagnetic Corrections and Pascal's Constants. *J. Chem. Educ.* **2008**, 85, 532–536.
- (35) Data reproducibility was checked by susceptibility measurements on three independently synthesized samples of complex **2**.
- (36) Gambarotta, S.; Floriani, C.; Chiesi-Villa, A.; Guastini, C. Cyclopentadienyldichlorotitanium(III): A Free-Radical-like Reagent for Reducing –N=N– Multiple Bonds in Azo and Diazo Compounds. *J. Am. Chem. Soc.* **1983**, 105, 7295–7301.
- (37) A more recent X-ray crystal structure determination of $[\text{Ti}(\eta^5\text{-C}_5\text{H}_5)\text{Cl}_2(\text{thf})_2]$ has been reported: Hamilton, E. J. M.; Park, J. S.; Chen, X.; Liu, S.; Sturgeon, M. R.; Meyers, E. A.; Shore, S. G. β -Agostic Interactions in 15-Valence-Electron 9-BBN Hydroborate Half-Sandwich Titanium(III) Complexes. *Organometallics* **2009**, 28, 3973–3980.
- (38) The $[\{\text{Ti}(\eta^5\text{-C}_5\text{Me}_5)(\mu\text{-Cl})_2\}_2]$ complex in the triplet state is computed to be 1.6 kcal/mol thermodynamically less stable than the corresponding singlet shown in Scheme 2.
- (39) Basta, R.; Harvey, B. G.; Arif, A. M.; Ernst, R. D. Reactions of SF_6 with Organotitanium and Organozirconium Complexes: The “Inert” SF_6 as a Reactive Fluorinating Agent. *J. Am. Chem. Soc.* **2005**, 127, 11924–11925.
- (40) Erker, G.; Krüger, C.; Schlund, R. Synthese und Thermolyse von α -Titanocenyl-substituierten Dimethylethern: die überraschende Bildung von $[(\text{CH}_3\text{Cp})\text{Ti}(\text{OCH}_3)\text{Cl}]_4$. *Z. Naturforsch.* **1987**, 42B, 1009–1016.

-
- (41) The closed-shell singlet excited state is located 41.8 kcal/mol higher in energy at the optimized structure of the transition state.
- (42) Hidalgo Llinás, G.; Mena, M.; Palacios, F.; Royo, P.; Serrano, R. (C₅Me₅)SiMe₃ as a Mild and Effective Reagent for Transfer of the C₅Me₅ Ring: An Improved Route to Monopentamethylcyclopentadienyl Trihalides of the Group 4 Elements. *J. Organomet. Chem.* **1988**, *340*, 37–40.
- (43) Farrugia, L. J. *WinGX and ORTEP for Windows: An Update. J. Appl. Crystallogr.* **2012**, *45*, 849–854.
- (44) Sheldrick, G. M. *SHELXT – Integrated Space–Group and Crystal-Structure Determination. Acta Crystallogr., Sect. A* **2015**, *71*, 3–8.
- (45) Sheldrick, G. M. Crystal Structure Refinement with *SHELXL. Acta Crystallogr., Sect. C* **2015**, *71*, 3–8.
- (46) (a) Adamo, C.; Barone, V. Toward Reliable Density Functional Methods without Adjustable Parameters: The PBE0 Model. *J. Chem. Phys.* **1999**, *110*, 6158–6169. (b) Ernzerhof, M.; Scuseria, G. E. Assessment of the Perdew–Burke–Ernzerhof Exchange–Correlation Functional. *J. Chem. Phys.* **1999**, *110*, 5029–5036.
- (47) Grimme, S.; Ehrlich, S.; Goerigk, L. Effect of the Damping Function in Dispersion Corrected Density Functional Theory. *J. Comput. Chem.* **2011**, *32*, 1456–1465.
- (48) Weigend, F.; Ahlrichs, R. Balanced Basis Sets of Split Valence, Triple Zeta Valence and Quadruple Zeta Valence Quality for H to Rn: Design and Assessment of Accuracy. *Phys. Chem. Chem. Phys.* **2005**, 3297–3305.
- (49) (a) Noodleman, L. Valence Bond Description of Antiferromagnetic Coupling in Transition Metal Dimers. *J. Chem. Phys.* **1981**, *74*, 5737–5743. (b) Noodleman, L.; Davidson, E. R.

Ligand Spin Polarization and Antiferromagnetic Coupling in Transition Metal Dimers.
Chem. Phys. **1986**, *109*, 131–143.

- (50) (a) Yamaguchi, K.; Takahara, Y.; Fueno, T. Ab-Initio Molecular Orbital Studies of Structure and Reactivity of Transition Metal-OXO Compounds in Smith, V. H.; Schaefer, H. F.; Morokuma, K. (Eds.) *Applied Quantum Chemistry*; Springer: Dordrecht, The Netherlands, **1986**, 155–184. (b) Soda, T.; Kitagawa, Y.; Onishi, T.; Takano, Y.; Shigeta, Y.; Nagao, H.; Yoshioka, Y.; Yamaguchi, K. Ab Initio Computations of Effective Exchange Integrals for H–H, H–He–H and Mn₂O₂ Complex: Comparison of Broken-Symmetry Approaches. *Chem. Phys. Lett.* **2000**, *319*, 223–230.
- (51) (a) Becke, A. D. Density-Functional Thermochemistry. III. The Role of Exact Exchange. *J. Chem. Phys.* **1993**, *98*, 5648–5652. (b) Lee, C.; Yang, W.; Parr, R. G. Development of the Colle-Salvetti Correlation-Energy Formula into a Functional of the Electron Density. *Phys. Rev. B* **1988**, *37*, 785–789. (c) Stephens, P. J.; Devlin, F. J.; Chabalowski, C. F.; Frisch, M. J. Ab Initio Calculation of Vibrational Absorption and Circular Dichroism Spectra Using Density Functional Force Fields. *J. Phys. Chem.* **1994**, *98*, 11623–11627.
- (52) Gaussian 16, Revision B.01, Frisch, M. J.; Trucks, G. W.; Schlegel, H. B.; Scuseria, G. E.; Robb, M. A.; Cheeseman, J. R.; Scalmani, G.; Barone, V.; Petersson, G. A.; Nakatsuji, H.; Li, X.; Caricato, M.; Marenich, A. V.; Bloino, J.; Janesko, B. G.; Gomperts, R.; Mennucci, B.; Hratchian, H. P.; Ortiz, J. V.; Izmaylov, A. F.; Sonnenberg, J. L.; Williams-Young, D.; Ding, F.; Lipparini, F.; Egidi, F.; Goings, J.; Peng, B.; Petrone, A.; Henderson, T.; Ranasinghe, D.; Zakrzewski, V. G.; Gao, J.; Rega, N.; Zheng, G.; Liang, W.; Hada, M.; Ehara, M.; Toyota, K.; Fukuda, R.; Hasegawa, J.; Ishida, M.; Nakajima, T.; Honda, Y.; Kitao, O.; Nakai, H.; Vreven, T.; Throssell, K.; Montgomery, Jr., J. A.; Peralta, J. E.; Ogliaro, F.; Bearpark, M. J.; Heyd, J. J.; Brothers, E. N.; Kudin, K. N.; Staroverov, V. N.;

Keith, T. A.; Kobayashi, R.; Normand, J.; Raghavachari, K.; Rendell, A. P.; Burant, J. C.; Iyengar, S. S.; Tomasi, J.; Cossi, M.; Millam, J. M.; Klene, M.; Adamo, C.; Cammi, R.; Ochterski, J. W.; Martin, R. L.; Morokuma, K.; Farkas, O.; Foresman, J. B.; Fox, D. J. Gaussian, Inc., Wallingford CT, 2016.

- (53) Aquilante, F.; Autschbach, J.; Carlson, R. K.; Chibotaru, L. F.; Delcey, M. G.; De Vico, L.; Fdez. Galván, I.; Ferré, N.; Frutos, L. M.; Gagliardi, L.; Garavelli, M.; Giussani, A.; Hoyer, C. E.; Li Manni, G.; Lischka, H.; Ma, D.; Malmqvist, P. Å.; Müller, T.; Nenov, A.; Olivucci, M.; Pedersen, T. B.; Peng, D.; Plasser, F.; Pritchard, B.; Reiher, M.; Rivalta, I.; Schapiro, I.; Segarra-Martí, J.; Stenrup, M.; Truhlar, D. G.; Ungur, L.; Valentini, A.; Vancoillie, S.; Veryazov, V.; Vysotskiy, V. P.; Weingart, O.; Zapata, F.; Lindh, R. MOLCAS 8: New Capabilities for Multiconfigurational Quantum Chemical Calculations Across the Periodic Table. *J. Comput. Chem.* **2016**, *37*, 506–541.